Bulletin of the Seismological Society of America, Vol. 103, No. 3, pp. 2062–2069, June 2013, doi: 10.1785/0120120279

Is the Initial Thermal State of a Fault Relevant to its Dynamic Behavior?

by Andrea Bizzarri and Paola Crupi

Abstract The prediction of impending earthquakes undoubtedly remains one of the most pursued goals of modern seismology. Within the framework of a deterministic description of earthquake faulting, the initial state of the fault system and the choice of the governing model describing its rheological behavior play a fundamental role in the description of the earthquake recurrence. In classical models of faulting, this initial state is basically described by the initial shear-stress distribution (prior to the next earthquake event) and by the initial sliding velocity. In this paper, by assuming a rate-, state-, and temperature-dependent rheology, we investigate whether the initial thermal state of the fault can also have a significant role in earthquake dynamics. Our numerical results clearly demonstrate that the initial temperature greatly influences the cosesimic slip (and thus the earthquake magnitude), the released stress (and thus the radiated energy), and the interevent time (i.e., the earthquake recurrence). Despite the remaining issues on the concept of earthquake cyclicity, our results can contribute to the lively debate on the deterministic hazard assessment, illuminating that the temperature field also plays a fundamental role in earthquake dynamics, not only because it controls possible phase changes and the chemical environment of the fault zone, but also because it affects the response of a brittle fault and earthquake cycles.

Introduction

In recent years, a large emphasis has been placed on the thermal properties of the fault zones, as well as on the potential role of the temperature during cosesimic slip (e.g., Chester and Higgs, 1992; Fialko, 2004). The seminal paper on the heat-flux paradox by Lachenbruch (1980) and the apparent scarcity of pseudotachylytes (Sibson, 2003; see also Kirkpatrick *et al.*, 2009) motivated studies modeling the frictional heat produced during seismic sliding. Recent theoretical studies on the spontaneous propagation of earthquake ruptures on 3D faults revealed that melting of rocks and fault gouge is likely to occur even with the inclusion of the thermal pressurization of pore fluids (Bizzarri and Cocco, 2006a,b). Moreover, the dramatic fault weakening at high slip rates predicted by the flash heating of microasperity contacts is not able to avert melting (Bizzarri, 2009). Despite the large number of fault-governing models presented in the literature (see Bizzarri, 2011c for a thorough review), the only constitutive law able to avoid the melting is a slip- and velocity-weakening friction law (Sone and Shimamoto, 2009; Bizzarri, 2010a), for which the fault weakening is so dramatic that it cannot be counterbalanced by the resulting enhanced slip velocities. Indeed, both thermal pressurization of pore fluids and flash heating predict not only a very dramatic stress drop, but also a very high peak in fault slip velocity, so that the final result is that melting temperature is very often exceeded, unless the slipping zone (where the deformation is concentrated) is extremely large (Bizzarri and Cocco, 2006b; Bizzarri, 2009). When melting occurs, the rheological behavior of the fault zone no longer obeys the Coulomb–Amonton–Mohr formulation, in that a viscous rheology is needed to describe the traction evolution during the ongoing rupture propagation (see Bizzarri, 2011a, and references cited therein).

It is well known that the initial state of a fault, expressed in terms of the sliding velocity (v_0) and shear distribution (τ_0), plays a fundamental role in predicting the behavior of that fault (e.g., the time occurrence of an instability), and, at the same time, it represents the most serious limitation in a deterministic approach to describing the earthquake faulting mechanisms (Bizzarri, 2012). The main aim of the present paper is to explore whether the initial thermal state of the fault (namely the initial temperature T_0) also plays an important role in the determination of repeated slip failures on the same seismogenic structure and in the overall dynamics of the fault.

Methodology

In this paper we employ the same fault model considered in Crupi and Bizzarri (2013); we simulate the traction evolution on the fault surface by adopting the simple one-degree-of-freedom spring-slider analog fault system, described by the following equation of motion:

$$m\ddot{u} = kv_{\text{load}}t - ku - \tau - c\dot{u}, \tag{1}$$

In equation (1), m is the mass (per unit surface) of the fault, k is the elastic constant of the spring (mimicking the elastic behavior of the medium in which the fault is embedded), v_{load} is the loading velocity (which basically expresses the loading rate of tectonic origin acting in the considered fault system), t is the time, u is the displacement (which in more elaborated continuum models is the fault slip, i.e., the displacement discontinuity across the fault interface; Bizzarri and Cocco, 2005) and τ is the frictional resistance (which is analytically expressed by the adopted governing model). Moreover, the overdots represent the time derivative of u, and the last term appearing in (1) is the so-called radiation-damping term (which represents the energy lost during the sliding in terms of propagating seismic waves; Rice, 1993). The quantity c is a constant, depending on the rigidity of the elastic medium (G) and on its S-wave velocity (v_S) ($c \equiv \frac{G}{2v_S}$).

The equation of motion (1) is complemented by the fault-governing model; here we assume the following version of a rate- and state-dependent friction law:

$$\begin{cases} \tau = \left[\mu_* + a\ln\left(\frac{v}{v_*}\right) + b\ln\left(\frac{\Psi v_*}{L}\right) + \frac{aQ_a}{R}\left(\frac{1}{T} - \frac{1}{T_*}\right)\right]\sigma_n^{\text{eff}} \\ \frac{\mathrm{d}}{\mathrm{d}t}\Psi = -\frac{\Psi v}{L}\left[\ln\left(\frac{\Psi v}{L}\right) + \frac{Q_b}{R}\left(\frac{1}{T} - \frac{1}{T_*}\right)\right] \end{cases}. \tag{2}$$

Equation (2) can be regarded as a generalization of the Ruina–Dieterich (RD) model (Ruina, 1983) written as equation (39) in Bizzarri (2011c), which incorporates an explicit dependence on the absolute temperature T developed by frictional heat (Chester and Higgs, 1992), so that $\tau = \tau(v(t), \Psi(t), T(t))$. The present formulation is analogous to equation (48) in Bizzarri (2011c), which in turn is written for the state variable Θ of Ruina (1983) instead of the state variable Ψ of Dieterich (1978). These two state variables (Θ and Ψ) are intimately related (see equation 38 in Bizzarri, 2011c), so that the two formulations of the governing model are equivalent.

The basic physical foundation-governing model (2), which is empirical in its origin, is that an Arrhenious relationship of the form $\mathrm{d}(\ln(v))/\mathrm{d}(1/T) = -Q/R$ is attributed to the slip rate to describe the thermally activated micromechanisms during the coseismic slip. An alternative point of view is that of Nakatani (2001), who interpreted the dependence of the frictional resistance of the contacting interface on the temperature through a linear variation of the constitutive parameter a for the increasing temperature at contacts.

The quantities μ_* and v_* in equation (2) are reference values of the friction coefficient and of the sliding velocity, respectively; a and b are constitutive parameters that express the direct and the evolution effect of friction, respectively; and L is the characteristic distance for the state variable evolution. Moreover, σ_n^{eff} is the effective normal stress (assumed to be constant through time in this study); R is the universal gas constant; Q_a and Q_b are apparent activation energies pertaining to the direct and evolution effect respectively; and T_* is a reference value for the temperature T. In this paper, we assume that $T_* = T_0$ (i.e., the temperature at $t = 0$). We also assume that $Q_a = Q_b$, as previously done by Chester (1994), Blanpied *et al.* (1998), Kato (2001), and Bizzarri (2010b).

If we indicate with ΔT the temperature change ($\Delta T \equiv T - T_0$), the last term appearing in equation (2) can be conveniently written as

$$\left(\frac{1}{T} - \frac{1}{T_*}\right) = -\frac{\Delta T}{T_0(T_0 + \Delta T)} < 0, \tag{3}$$

which emphasizes the explicit dependencies of τ (and of Ψ) on both the initial temperature and the temperature change.

The temperature field is computed as follows (McKenzie and Brune, 1972; Kato, 2001):

$$T(t) = T_0 + \frac{1}{2C\sqrt{\pi\chi}}\int \frac{q(t')}{\sqrt{t - t'}}\,dt', \tag{4}$$

so that

$$\Delta T(t) = \frac{1}{2C\sqrt{\pi\chi}}\int \frac{q(t')}{\sqrt{t - t'}}\,dt', \tag{5}$$

where C is the heat capacity of the bulk composite for unit volume and χ is the thermal diffusivity.

The quantity q in equations (4) and (5) is the heat-input term, written as

$$q(t') = \tau(t')v(t'), \tag{6}$$

which accounts for the slip velocity and traction histories. As discussed by Bizzarri (2010c), equations (4) and (6) are known to maximize the effects of the frictional heat, compared to other models that incorporate a characteristic length of the fault thickness (Fialko, 2004; Bizzarri and Cocco, 2006a,b). Indeed, in the present paper, we use an infinitesimal fault zone, which assumes that all the deformation (and the temperature change) is confined in a mathematical fault plane. The solution of the problem (coupled equations 1, 2, and 5) is obtained numerically, as described in detail in Bizzarri (2012; his section 2.3).

Simulation Results

As clearly stated by equation (5), ΔT does not depend on T_0, but only on the fault dynamics (namely, it depends on the time evolutions of v and τ). In this case, T_0 represents only a shift of the temperature change produced during sliding, and therefore T_0 is important only because it contributes to determining the actual temperature, which in turn can eventually exceed the melting temperature (and thus lead to phase change, as discussed in the Introduction) and can also control the chemical environment (i.e., it can induce thermally activated chemical reactions). Some examples are the thermochemical pressurization of pore fluids (Brantut

et al., 2010), in which mineral dehydration reactions are triggered by temperature changes, and the thermal carbonate decomposition (Han *et al.*, 2007, 2010), observed at high speeds.

The situation is more complicated when ΔT depends on T_0. Indeed, the governing model considered here (equation 2) explicitly depends on the initial temperature, as stated by (3). In turn, this reflects a dependence of the heat-input term q on T_0 (see equation 6), which finally gives a dependence of ΔT on T_0 (see equation 5). In other words, because the rheology is assumed to depend on T_0 (which mathematically represents the third initial condition for the system, in addition to the initial sliding speed and to the initial value of the state variable), the temperature change will depend on T_0.

In this section, we explore the effects of the variations of T_0 on the resulting dynamics of a fault governed by equation (2). The reference parameters are tabulated in Table 1. In Figure 1 we report the numerical results pertaining to three different configurations, the reference one (black curve) and two additional situations having different T_0. It is apparent that the overall behavior of the simulated seismicity is affected by the choice of the initial temperature field; the slip cumulated during each slip failure (Fig. 1a), the velocity peaks (Fig. 1b), the minima of velocity (Fig. 1c), the failure stress points, and the minima of stress (Fig. 1d) are quite different. As a consequence of the different velocity and stress histories in the various configurations, the temperature change due to frictional heat is different for the various values of T_0, as shown in Figure 2. We observe that the simulated temperature changes are not proportional to T_0; for the parameters adopted here we have $\Delta T^{(T_0=55°C)} < \Delta T^{(T_0=100°C)} < \Delta T^{(T_0=40°C)}$.

Figure 3 shows the phase portrait, which reports the (normalized) traction versus the (logarithm of the normalized) velocity. We can clearly see that the upper yield stress, which formally represents the instant when the stress-release process begins, is different in the three considered scenarios, as also shown in Figure 1d. The dependence of the direct effect on ΔT is not surprising; if we arrange the first equation of (2) we can write

$$\tau = \left[\mu_* + a\ln\left(\frac{v}{v_*}\right)\left(1 - \frac{\frac{Q_a \Delta T}{RT_0(T_0+\Delta T)}}{\ln\left(\frac{v}{v_*}\right)}\right) + b\ln\left(\frac{\Psi v_*}{L}\right)\right]\sigma_n^{\text{eff}}. \tag{7}$$

Remarkably, if we neglect the temperature dependence ($\Delta T = 0$), from (7) it emerges that the direct effect simply reduces to the canonical term $a\ln(\frac{v}{v_*})$, which characterizes the classical RD model (Ruina, 1983). Consequently, assuming $\Delta T = 0$, the Chester and Higgs (CH) law becomes exactly the RD constitutive law, from which it differs just for the temperature dependence of friction. The dependence of the interseismic recovery stage is not only on T_0, but also on ΔT; indeed, we can see from Figure 3 that the amount of stress ($\Delta\tau_{\text{rec}}$) that the fault has to recover to produce a new slip failure (a new earthquake) is not directly proportional to the initial temperature. We have $\Delta\tau_{\text{rec}}^{(T_0=55°\,\text{C})} < \Delta\tau_{\text{rec}}^{(T_0=40°\,\text{C})} < \Delta\tau_{\text{rec}}^{(T_0=100°\,\text{C})}$. The quantity $\Delta\tau_{\text{rec}}$ is marked by dashed lines with arrows in Figure 1d. One interesting thing emerging from Figure 3 is that the recovery stage does not have the same slope for the three cases. Indeed, in the traction–time diagram (Fig. 1d), the slope is the same, because it is basically controlled by the external loading rate, which is the same for all three simulations. On the contrary, in the traction–velocity diagram (Fig. 3), the slope is different, because it is controlled by the location of the point when the velocity is minimum and when the traction is maximum; both these points depend on the time evolution of the system and not merely on the externally imposed conditions.

For all the simulations reported here (and for the other cases considered in Figs. 4 and 5) we emphasize that the phase portrait is always characterized by the "8-shaped" trajectory, previously found in Crupi and Bizzarri (2013). Readers can refer to that paper for a detailed discussion. Here we simply recall that this kind of behavior essentially represents a fast restrengthening stage occurring just after the dynamic breakdown and the stress-release process, during which the frictional resistance increases due to the presence of the explicit dependence on the temperature. This behavior,

Table 1
Reference Parameters Adopted in This Paper

Parameter	Value
Loading velocity, v_{load}	3.17×10^{-10} m/s (= 10 mm/yr)
Machine stiffness, k	10 MPa/m
Tectonic loading rate, $\dot{\tau}_0 = kv_{\text{load}}$	3.17×10^{-3} Pa/s (= 1 bar/yr)
Period of the analog freely slipping system, $T_{\text{a.f.}} = 2\pi\sqrt{m/k}$	5 s
Rigidity of the elastic medium, G	27 GPa
S-wave velocity, v_S	3 km/s
Cubic mass density, ρ	3000 kg/m^3
Radiation damping constant, c	4.5×10^6 Pa s/m
Effective normal stress, σ_n^{eff}	30 MPa
Initial sliding velocity, v_0	3.17×10^{-10} m/s ($= v_{\text{load}}$)
Initial state variable, Ψ_0	3.15×10^7 s ($= L/v_0$)
Initial shear stress, τ_0	16.8 MPa ($= \mu_* \sigma_n^{\text{eff}}$)
Initial temperature, T_0 (reference)	328.15 K (= 55°C)
Logarithmic direct-effect parameter, a	0.008
Evolution-effect parameter, b	0.016
Characteristic scale length, L	1×10^{-2} m
Reference value of friction coefficient, μ_*	0.56
Reference value of the sliding velocity, v_*	3.17×10^{-10} m/s ($= v_0$)
Activation energies, Q_a and Q_b	1×10^5 J/mol$^{(b)}$
Heat capacity for unit volume of the bulk composite, C	3×10^6 J/(m^3 K)
Thermal diffusivity, χ	1×10^{-6} m^2/s

The initial conditions (denoted by the subscript 0) refer to $t = 0$. The values of σ_n^{eff} and T_0 pertain to a reference hypocentral depth roughly of 1.5 km, if we assume lithostatic and hydrostatic stresses and a typical geothermal gradient of 30°C/km (with a ground temperature equal to 10° C).

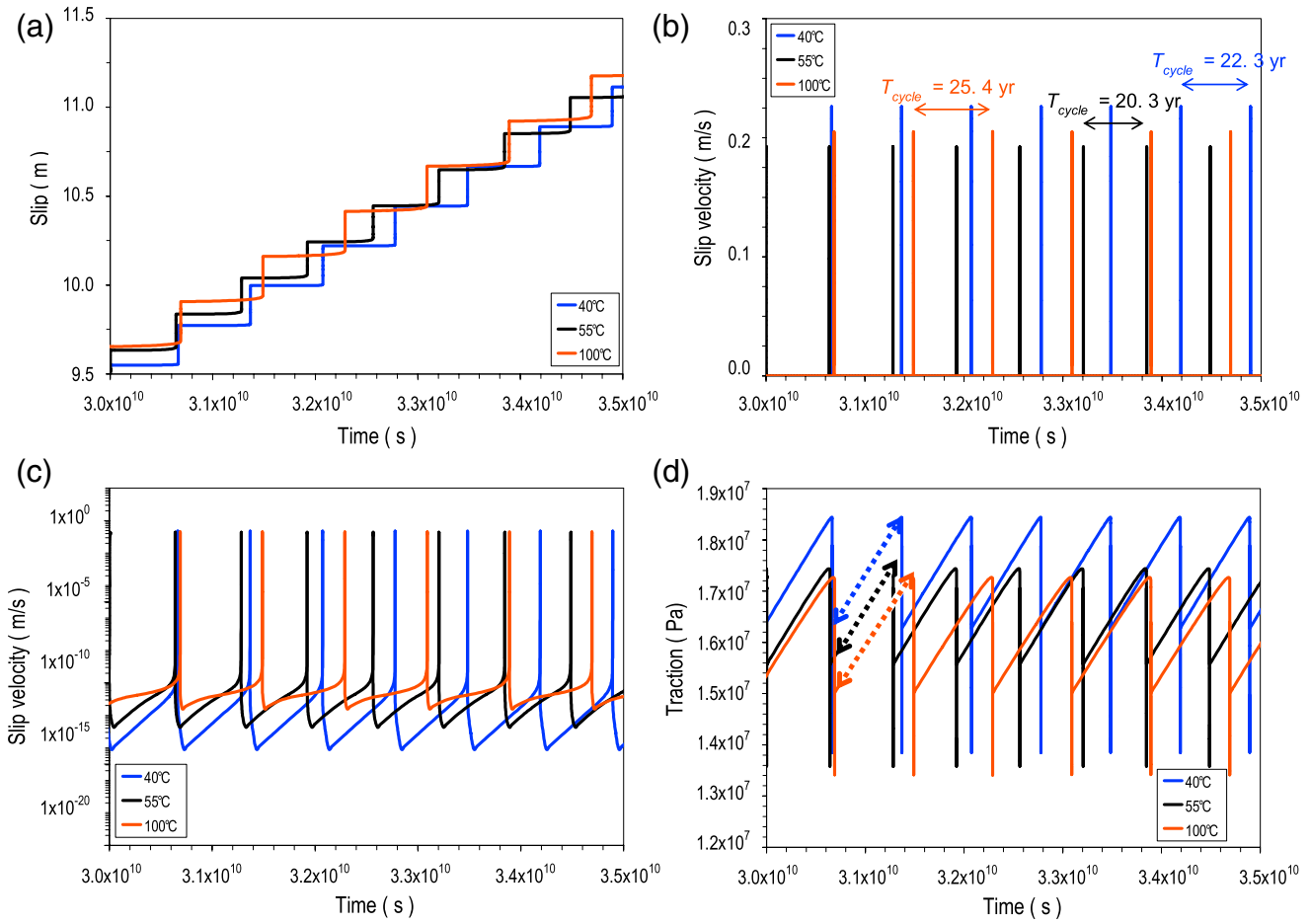

Figure 1. Numerical results for a single-degree-of-freedom spring-slider system governed by the CH law (coupled equations 1 and 2) for three different initial temperatures and for the reference parameters listed in Table 1. (a) Time history of slip. (b) Time history of slip velocity. The resulting value of the interevent time is reported for the three cases. (c) The same as panel (b), but now in a semilogarithmic scale. (d) Traction evolution. The dashed lines with arrows in panel (d) represent the stages when the ruptures recover the amount of stress $\Delta\tau_{rec}$ marked in Figure 3. In all panels, we selected a time interval of the whole life of the fault in order to emphasize the different resulting recurrence times. The color version of this figure is available only in the electronic edition.

which results in a switch from clockwise to counterclockwise direction of the trajectory, is intimately related to the fast restrengthening stage, which characterizes the CH law, as pointed out in 3D by Bizzarri (2010b); just after the stress drop occurring in the breakdown stage, the traction is partially recovered and healing occurs. Interestingly, the absolute minimum attained by the traction after the dynamic stress drop is roughly the same in all cases, but the value of τ corresponding to the decelerating stage of the phase portrait (bottom horizontal part of the trajectory) is not the same; in addition to the change in the upper yield stress, this dissimilarity causes $\Delta\tau_{rec}$ to be different in the three simulations reported.

Influence of T_0 on Earthquake Cycles

We have seen in the Simulation Results section that the initial temperature field affects the dynamics of the fault in terms of developed slip (which is related to the magnitude of the event in a more elaborated, extended fault model), slip velocity, as well as traction history. T_0 also influences the time occurrence of the slip failure, that is, the seismic cycle (T_{cycle}). The latter is defined as the interval that separates two subsequent instabilities, marked by the time when v first exceeds the threshold value v_l. We perform a series of numerical experiments by considering different values of the effective normal stress and model's parameters; the results are plotted in Figure 4.

As expected, if the RD model is assumed to govern the system, the simulated T_{cycle} does not depend on T_0 (open black squares in Fig. 4). On the contrary, when the CH governing model is assumed, T_{cycle} is significantly controlled by the initial temperature. For an example, in the case with $c = 5.26 \times 10^6$ Pa s/m (open blue circles in Fig. 4) we have a variation roughly of -240% in T_{cycle} by changing from $T_0 = 40°\,\mathrm{C}$ to $T_0 = 100°\,\mathrm{C}$ (T_{cycle} equals 58 yr and 24 yr, respectively) and a variation roughly of $+310\%$ in T_{cycle} by changing from $T_0 = 100°\,\mathrm{C}$ to $T_0 = 600°\,\mathrm{C}$ (T_{cycle} equals 24 yr and 74 yr, respectively).

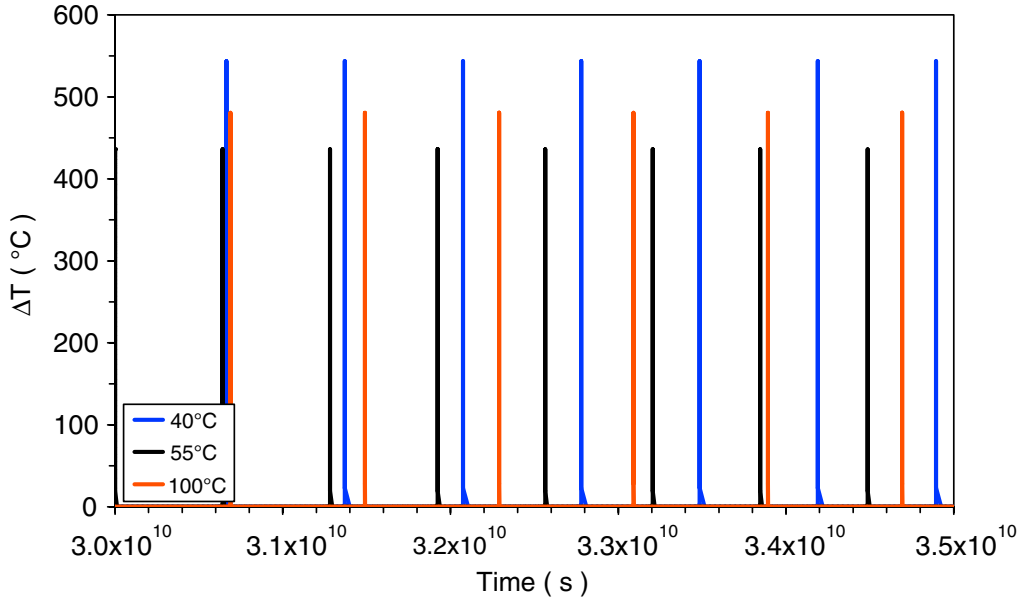

Figure 2. Time evolution of the temperature change (as computed from equation 5) for the various cases reported in Figure 1. The color version of this figure is available only in the electronic edition.

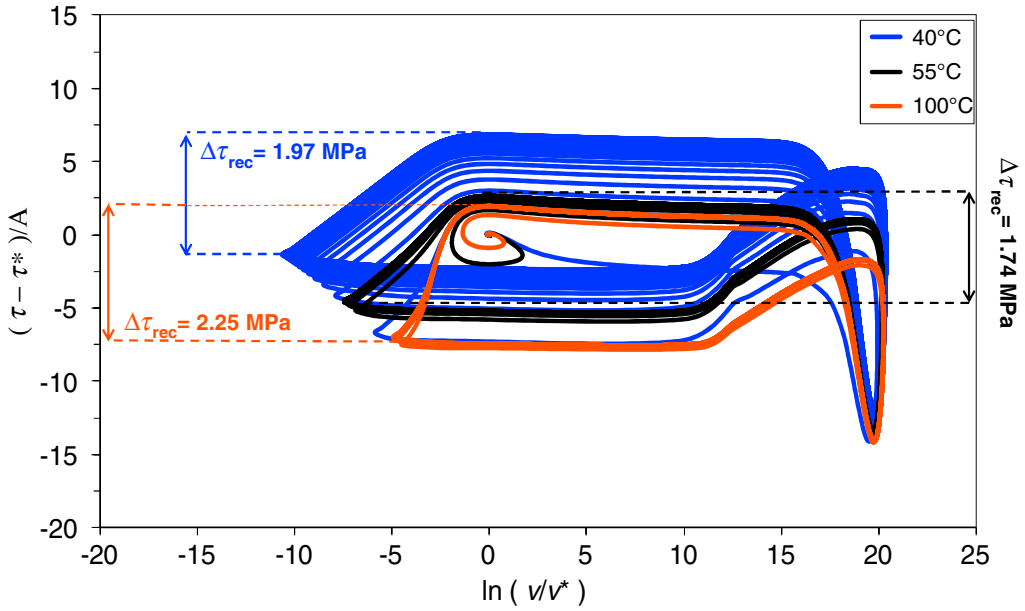

Figure 3. Phase portrait (i.e., normalized traction versus velocity) for the various cases of Figure 1. The traction difference is normalized by the quantity $A = a\sigma_n^{\text{eff}}$. The values of the amount of stress that the fault has to recover in order to reach produce a new instability are indicated for the various situations. The color version of this figure is available only in the electronic edition.

One of the most interesting results emerging from these simulations is that T_{cycle} does not exhibit a linear proportionality with T_0, but it has a minimum (which is marked by a vertical line for the various configurations). The values of the initial temperature at which this minimum is realized (a critical temperature) does not always correspond to the temperature predicted by the geothermal gradient (which is denoted by big symbols in Fig. 4). This trend is a general feature of the CH law, which appears for all the configurations explored, and it is also maintained for higher effective normal stress, not reported here, for which the resulting temperature change is very high. In the context of hazard assessment, this result is important, because it tells us that T_0 can affect the recurrence time, and that it does so in a complicated way.

The presence of a local minimum T_{cycle} seen from Figure 4 can be physically interpreted by considering the restrengthening stage of the rupture. Indeed, in Figure 4 the three full black circles before, at, and after the minimum

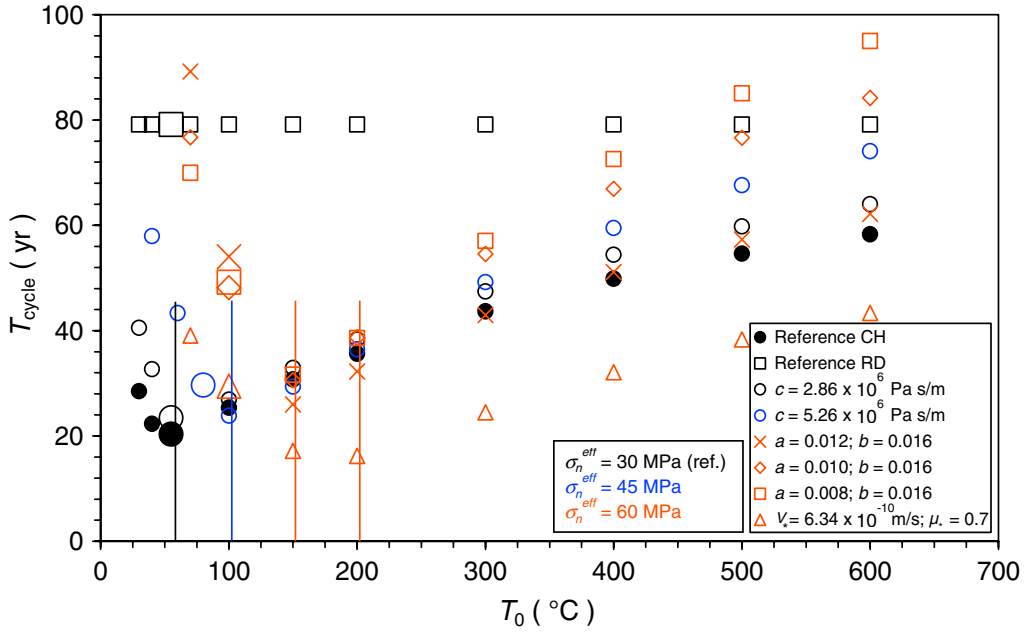

Figure 4. Behavior of the interevent time (i.e., the cycle time T_{cycle}) as a function of the assumed initial temperature field. Different values of the effective normal stress are denoted by different colors, reported in the legend. In black, we plot the reference configuration of Table 1 for both the CH law (full circles) and the RD law (open squares). The vertical lines emphasize, for the different cases, the initial temperature, which corresponds to the minimum of T_{cycle} (i.e., the critical temperature). The big symbols denote the temperatures corresponding to the geothermal profiles at the hypocentral depths defined by the assumed values of σ_n^{eff}. The color version of this figure is available only in the electronic edition.

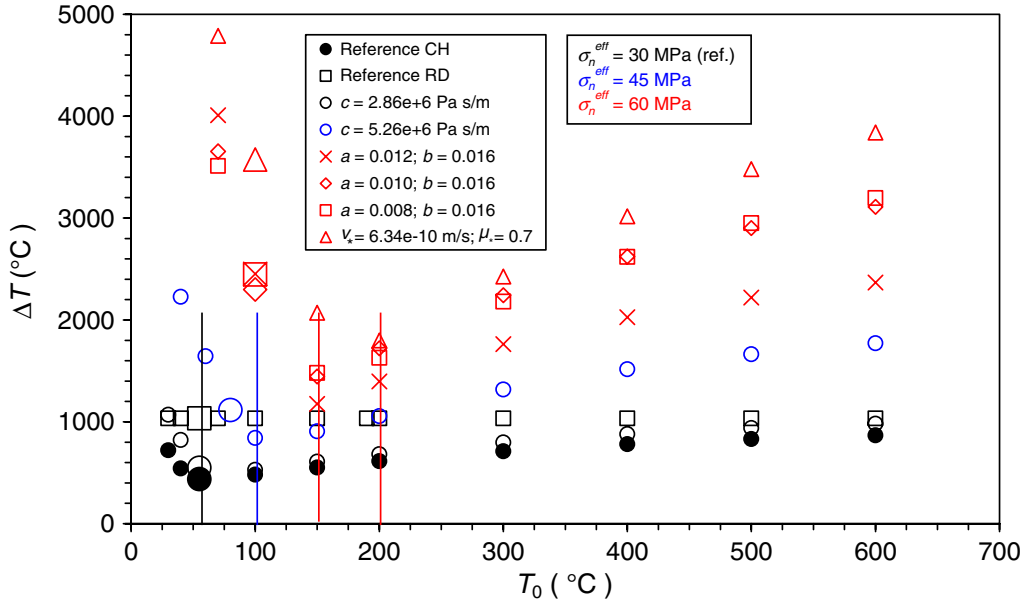

Figure 5. Temperature variation as a function of T_0. The plotting strategies are the same as in Figure 4. We also note the presence of a minimum in ΔT for all the configurations considered. The color version of this figure is available only in the electronic edition.

in T_{cycle} represent the simulations presented in Figures 1–3. We can see that $T_{cycle}^{(T_0=55^\circ C)} < T_{cycle}^{(T_0=40^\circ C)} < T_{cycle}^{(T_0=100^\circ C)}$. This sequence is exactly that we observe in $\Delta\tau_{rec}$ (Fig. 3).

In general, the ΔT is proportional to the effective normal stress, as theoretically expected (see equations 5 and 6). Remarkably, it is apparent from Figure 5 that, except for the RD, which predicts a constant temperature change, regardless of the initial thermal state of the fault, ΔT explicitly depends on T_0 in the CH models (as also previously shown in Fig. 2). This dependence is nonlinear, and it is more pronounced at low temperatures (i.e., below the critical temperature); interestingly for low T_0 we have greater ΔT

compared to those obtained at high T_0. The important result is that, as for T_{cycle}, there is a critical value of the initial temperature which minimizes ΔT, and this critical value is the same value that minimizes the recurrence time.

From Figure 5 we can also see that ΔT predicted by the CH law (full black circles) approaches that predicted by the RD law for high values of T_0; this is expected from the theory (see equation 3). For the adopted parameters (Table 1), for $T_0 > 1000°$ C the temperature changes resulting from the CH and the RD law are nearly identical, as well as T_{cycle}. The same holds at low initial temperatures (i.e., for T_0 lower than the critical temperature that gives the minimum in ΔT). Again, for the parameters of Table 1, $\Delta T^{(CH)} \cong \Delta T^{(RD)}$ for $T_0 \sim 15°$ C. However, in this case $T_{cycle}^{(CH)} \neq T_{cycle}^{(RD)}$. It should be remarked that the temperature changes obtained from the models can eventually exceed the melting temperature, above which the Coulomb friction is no longer valid and a completely viscous rheology has to be considered. Melting temperature depends on the material composing the fault zone, and we can in general estimate an effective melting temperature (i.e., the threshold above which the purely brittle rheology is no longer applicable) between 1000° C and 2000° C (see Spry, 1969; Sibson, 1975; Bizzarri, 2011a; and references cited therein). Moreover, we recall that our calculation of the temperature T, equations (4) and (6), represents an upper bound of the frictional heat, which would be smaller if we introduce a thickness of the fault zone (e.g., Fialko, 2004). In any case, the behavior discussed above is clearly visible even below 1000° C.

Discussion and Concluding Remarks

The initial sliding velocity and the initial shear distribution play a fundamental role in predicting the time occurrence of earthquake instabilities and, at the same time, they represent the most relevant limitation in the framework of a deterministic description of earthquake faulting (see the discussion in Bizzarri, 2012). In this study, we explore whether the initial temperature field (T_0) has a role in the dynamics of a fault zone.

In a very general context, when the frictional heat (equation 6) causes an increase in temperature with respect to its initial condition, than T_0 is important because it controls the possible melting process; the higher T_0 is the more likely melting seems to occur (for a given frictional heat produced during sliding). Things are more complicated when the rheology explicitly depends on the temperature field ($T = T_0 + \Delta T$). This dependence has been incorporated into the framework of the rate- and state-dependent friction laws in two different ways, the first being the assumption that the so-called direct effect of friction explicitly depends on T (namely, when $a = a(T)$; see Bizzarri, 2011b, and references therein), and the second being the rate-, state-, and temperature-dependent rheology (the Chester-Higgs constitutive model; Chester and Higgs, 1992).

In this paper, we consider a simple 1D spring-slider fault model, and we assume the second approach. We are aware that the empirical model adopted here has been retrieved in laboratory conditions and that the extension of such laboratory results to real-world scale is somehow problematic, because the rate dependence of friction changes with temperature and only a limited range of sliding speed (and confining stress) can be accessed during laboratory experiments.

One outcome of the present study is that the simulated earthquakes explicitly depend on the assumed initial thermal state of the fault, in that the developed slip (and thus the magnitude of the events) is different (see Fig. 1a), as well as the stress drop (see Figs. 1d and 3). By changing T_0 we have different velocity and traction histories (see Fig. 1b–d), which in turn cause different values of the temperature change ΔT (see Fig. 2). Finally, this affects the traction evolution during the subsequent failure events, as stated by equation (7). In other words, we can say that the fault behaves differently depending on its initial thermal state.

One of the consequences of this result is that the dependence of the earthquake cyclicity on the seismogenic depth is twofold; the effective normal stress explicitly controls the frictional resistance (which in the brittle regime is $\tau = \mu\sigma_n^{eff}$), but also the initial temperature (which of course depends on the geothermal gradient) controls the dynamic behavior of the fault.

A prominent result highlighted by our numerical simulations is that the interevent time (T_{cycle}) also depends on the thermal state of the fault; Figure 4 clearly shows a persistent feature of the CH law (i.e., T_{cycle} is not merely controlled by the governing parameters, such as a, b, L, and the external conditions, but also on T_0). This argument suggests that the empirical relation found by Lapusta and Barbot (2012, their equation 24) is valid only in the framework of the canonical formulation of the rate- and state-dependent friction laws.

Moreover, all the scenarios explored here indicate that there exists an initial temperature that minimizes T_{cycle}. The presence of this minimum (also identified for ΔT, as discussed in the Influence of T_0 on Earthquake Cycles section) is not *a priori* predictable from equation (2), because the problem is nonlinear and only numerical simulations can provide such a result. Interestingly, this critical temperature does not always coincide with the temperature predicted by the geothermal gradient. In general, we can observe a decreasing seismic cycle for low values of T_0 and then an increasing interevent times for high values of the initial temperature. The minimum is controlled by the amount of stress $\Delta\tau_{rec}$ that the fault has to recover to reach again the yield point (Fig. 3).

Given the intrinsic limitations of the adopted fault model, which however is certainly able to capture the first order of approximation the behavior of a natural fault, the results found here are relevant in the context of seismic hazard assessment. If it is true that the rheology of a seismic fault is explicitly controlled by the temperature, as the laboratory experiments tend to suggest, then the initial thermal state of a fault directly controls the time evolution of a seismogenic

fault. Moreover, T_0 finally controls the recurrence times, and not in a simple way.

Data and Resources

All data sources were taken from published works listed in the References.

Acknowledgments

The authors wish to thank Associate Editor D. D. Oglesby and two anonymous referees for the stimulating and very constructive comments that contributed to improving the paper.

References

Bizzarri, A. (2009). Can flash heating of asperity contacts prevent melting? *Geophys. Res. Lett.* **36,** L11304, doi: 10.1029/2009GL037335.

Bizzarri, A. (2010a). An efficient mechanism to avert frictional melts during seismic ruptures, *Earth Planet. Sci. Lett.* **296,** 144–152, doi: 10.1016/j.epsl.2010.05.012.

Bizzarri, A. (2010b). Pulse-like dynamic earthquake rupture propagation under rate-, state-, and temperature-dependent friction, *Geophys. Res. Lett.* **37,** L18307, doi: 10.1029/2010GL044541.

Bizzarri, A. (2010c). Determination of the temperature field due to frictional heating on a sliding interface, *I.N.G.V. Technical Reports* **158,** 1–16, http://istituto.ingv.it/l-ingv/produzione-scientifica/rapporti-tecnici-ingv/archivio/rapporti-tecnici-2010/ (last accessed March 2013).

Bizzarri, A. (2011a). Dynamic seismic ruptures on melting fault zones, *J. Geophys. Res.* **116,** B02310, doi: 10.1029/2010JB007724.

Bizzarri, A. (2011b). Temperature variations of constitutive parameters can significantly affect the fault dynamics, *Earth Planet. Sci. Lett.* **306,** 272–278, doi: 10.1016/j.epsl.2011.04.009.

Bizzarri, A. (2011c). On the deterministic description of earthquakes, *Rev. Geophys.* **49,** RG3002, doi: 10.1029/2011RG000356.

Bizzarri, A. (2012). What can physical source models tell us about the recurrence time of earthquakes? *Earth Sci. Rev.* **115,** 304–318, doi: 10.1016/j.earscirev.2012.10.004.

Bizzarri, A., and M. Cocco (2005). 3D dynamic simulations of spontaneous rupture propagation governed by different constitutive laws with rake rotation allowed, *Ann. Geophys.* **48,** no. 2, 279–299.

Bizzarri, A., and M. Cocco (2006a). A thermal pressurization model for the spontaneous dynamic rupture propagation on a three-dimensional fault: 1. Methodological approach, *J. Geophys. Res.* **111,** B05303, doi: 10.1029/2005JB003862.

Bizzarri, A., and M. Cocco (2006b). A thermal pressurization model for the spontaneous dynamic rupture propagation on a three-dimensional fault: 2. Traction evolution and dynamic parameters, *J. Geophys. Res.* **111,** B05304, doi: 10.1029/2005JB003864.

Blanpied, M. L., T. E. Tullis, and J. D. Weeks (1998). Effects of slip, slip rate, and shear heating on the friction of granite, *J. Geophys. Res.* **103,** 489–511, doi: 10.1029/97JB02480.

Brantut, N., A. Schubnel, J. Corvisier, and J. Sarout (2010). Thermochemical pressurization of faults during cosesimic slip, *J. Geophys. Res.* **115,** B05314, doi: 10.1029/2009JB006533.

Chester, F. M. (1994). Effects of temperature on friction: Constitutive equations and experiments with quartz gouge, *J. Geophys. Res.* **99,** 7247–7261, doi: 10.1029/93JB03110.

Chester, F. M., and H. G. Higgs (1992). Multimechanism friction constitutive model for ultrafine quartz gouge at hypocentral conditions, *J. Geophys. Res.* **97,** no. B2, 1859–1870.

Crupi, P., and A. Bizzarri (2013). The role of the radiation damping in the modeling of repeated earthquake events, *Ann. Geophys.* **56,** no. 1, doi: 10.4401/ag-6200.

Dieterich, J. H. (1978). Time-dependent friction and the mechanics of stick slip, *Pure Appl. Geophys.* **116,** 790–806, doi: 10.1007/BF00876539.

Fialko, Y. A. (2004). Temperature fields generated by the elastodynamic propagation of shear cracks in the Earth, *J. Geophys. Res.* **109,** B01303, doi: 10.1029/2003JB002497.

Han, R., T. Hirose, and T. Shimamoto (2010). Strong velocity weakening and powder lubrication of simulated carbonate faults at seismic slip rates, *J. Geophys. Res.* **115,** B03412, doi: 10.1029/2008JB006136.

Han, R., T. Shimamoto, T. Hirose, J.-H. Ree, and J.-i. Ando (2007). Ultralow friction of carbonate faults caused by thermal decomposition, *Science* **316,** no. 5826, 878–881.

Kato, N. (2001). Effect of frictional heating on preseismic sliding: A numerical simulation using a rate-, state-, and temperature-dependent friction law, *Geophys. J. Int.* **147,** 183–188.

Kirkpatrick, J. D., Z. K. Shipton, and C. Persano (2009). Pseudotachylytes: Rarely generated, rarely preserved, or rarely reported? *Bull. Seismol. Soc. Am.* **99,** no. 1, doi: 10.1785/0120080114.

Lachenbruch, A. H. (1980). Frictional heating, fluid pressure, and the resistance to fault motion, *J. Geophys. Res.* **85,** 6097–6122.

Lapusta, N., and S. Barbot (2012). Models of earthquakes and aseismic slip based on laboratory-derived rate and state friction laws, in *The Mechanics of Faulting: From Laboratory to Real Earthquakes*, A. Bizzarri and H. S. Bhat (Editors), 153–207, Ressign Post, ISBN: 978-81-308-0502-3, http://www.trnres.com/ebookcontents.php?id=122; http://www.trnres.com/ebook/uploads/bizzarric/T_13486559556%20Bizzari.pdf (last accessed March 2013).

McKenzie, D., and J. N. Brune (1972). Melting on fault planes during large earthquakes, *Geophys. J. R. Astr. Soc.* **29,** 65–78.

Nakatani, M. (2001). Conceptual and physical clarification of rate- and state-dependent friction law: Frictional sliding as a thermally activated rheology, *J. Geophys. Res.* **106,** 13,347–13,380, doi: 10.1029/2000JB900453.

Rice, J. R. (1993). Spatio-temporal complexity of slip on a fault, *J. Geophys. Res.* **98,** no. B6, 9885–9907.

Ruina, A. L. (1983). Slip instability and state variable friction laws, *J. Geophys. Res.* **88,** 10,359–10,370.

Sibson, R. H. (1975). Generation of pseudotachylytes by ancient seismic fault, *Geophys. J. R. Astron. Soc.* **43,** 775–794.

Sibson, R. H. (2003). Thickness of the seismic slip zone, *Bull. Seismol. Soc. Am.* **93,** no. 3, 1169–1178.

Sone, H., and T. Shimamoto (2009). Frictional resistance of faults during accelerating and decelerating earthquake slip, *Nat. Geosci.* **2,** 10, 705–708, doi: 10.1038/ngeo637.

Spry, A. (1969). *Metemorphic Textures*, Pergamon Press, Oxford and New York, 350 pp.

Istituto Nazionale di Geofisica e Vulcanologia
Sezione di Bologna, Italy
Via Donato Creti, 12
40128 Bologna, Italy
bizzarri@bo.ingv.it
(A.B.)

Università degli Studi di Bari
Dipartimento di Scienze della Terra e Geoambientali, Italy
Via Orabona 4
70125 Bari, Italy
paola.crupi@uniba.it
(P.C.)

Manuscript received 17 September 2012